Heat Transfer Research, 2009, Vol. 40, No. 6

The Overall Heat Transfer Characteristics of a Double-Pipe Heat Exchanger

A. R. ANSARI DEZFOLI* and M. A. MEHRABIAN

Department of Mechanical Engineering, Shahid Bahonar University of Kerman, P. O. Box 76175-133, Kerman, Iran

Heat exchangers are used in industrial processes to recover heat between two process fluids. The purpose of this paper is to develop analytical solutions using mathematical techniques to work out the two-dimensional (2D) temperature changes of flow in the passages of a double-pipe heat exchanger in parallel flow arrangement. Although the necessary equations for heat transfer in a double-pipe heat exchanger are available, using these equations the optimization of the system cost is laborious. Also, the solution of the problem yields the heat-transfer coefficient in inner and outer flows of double-pipe heat exchangers. The results are then compared with the experimental data available in other literature.

* * *

Key words: double-pipe heat exchanger; temperature distribution; parallel flow; counter flow; two-dimensional flow

INTRODUCTION

The simplest form of a two-fluid heat exchanger is a double-pipe heat exchanger made of two concentric circular tubes (see Fig. 1). The heat transfer characteristics and pressure drop for the flow through the circular tube and the concentric annular duct have been analyzed for a variety of boundary conditions [1, 2]. Abdelmessih and Bell [3] have taken a closer look to these exchangers recently. They found that both forced and natural convection contribute to the heat transfer process according to the following correlation:

*Corresponding author: A. R. Ansari Dezfoli, kadr_basteh@yahoo.com

 ISSN1064-2285

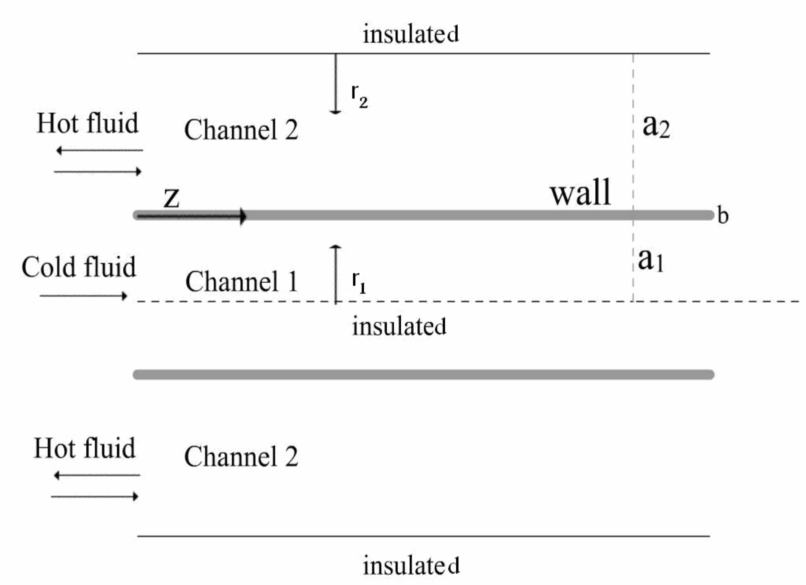

Fig. 1. Double-pipe heat exchanger.

$$Nu = \left[4.36 + 0.327\left(Gr\,\mathrm{Pr}\right)^{\frac{1}{4}}\right]\left(\frac{\mu_b}{\mu_w}\right)^{0.14}, \quad (1)$$

where all physical properties (except for μ_w) are evaluated at the local bulk temperature; Nu is the local peripheral average Nusselt number. The term representing the force convection effect (4.36) will be recognized as the result for a fully developed laminar flow with constant properties and a constant wall heat flux. The data used to generate Eq. (1) covered the following ranges:

$$120 \le \mathrm{Re} \le 2500 \quad , \quad 3.9 \le \mathrm{Pr} \le 110 \quad ,$$
$$2500 \le Gr \le 1130000 \quad , \quad 27 \le \frac{X}{d_i} \le 171. \quad (2)$$

Kays and Sellar [4] and Tribus and Klein [5] calculated the total and average Nusselt numbers for a laminar entrance region of a circular tube for the case of a fully developed velocity profile. The results of their analyses are shown as the variation of the average Nusselt number in terms of the inverse Graetz number [6]. The Sider–Tate [7] correlations have been used to design the double-pipe heat exchangers since 1950 and they are strongly recommended by Kern [8] in his old but reliable text. The Sieder–Tate [7] correlations can be used for predicting the film coefficients of flow in both the inner tube side and the outer tube side of a double-pipe heat exchanger. They can be used for both heating and cooling of a number of fluids, principally petroleum fractions, in horizontal and vertical tubes:

$$Nu = 1.86\,\mathrm{Re}^{\frac{1}{3}}\,\mathrm{Pr}^{\frac{1}{3}}\left(\frac{D}{L}\right)^{\frac{1}{3}}\left(\frac{\mu}{\mu_w}\right)^{0.14}. \quad (3)$$

The Sieder–Tate correlation is for an isothermal wall and is applied to a laminar flow (Re < 2100). Mehrabian and Mansouri [9] compared the outer and inner tube side heat-transfer coefficients deduced from experimental data with those evaluated on the basis of standard correlations. They showed that in the counter flow and parallel flow conditions, all standard correlations predict lower heat-transfer coefficients compared with experimental results. The outer tube side heat-transfer coefficients are smaller than the inner side heat-transfer coefficient by a factor of almost 1.5 and 3.4 in the counter flow and parallel flow arrangements, respectively. The agreement is very good for the counter flow arrangement, but not very good for the parallel flow arrangement. The main purpose of this paper is to conduct an introductory analytical investigation of temperature distribution and heat-transfer coefficients in double-pipe heat exchangers using the Sturm–Liouville problem. The temperature distribution in double-pipe heat exchangers is obtained based on a two-region Sturm--Liouville system consisting of two equations coupled at a common boundary. The solutions of this system form an infinite sequence of eigenfunctions with corresponding eigenvalues. The plug flow model of the heat exchanger fluid flows is utilized in this paper with the following idealizations:

1. At the inlet to the tube the temprature distributions within the fluids are constant.
2. Frictional heating is negligible.
3. Longitudinal heat conduction in the plates is negligible.
4. Physical properties are temperature independent.
5. Longitudinal heat conduction in the fluids is negligible.
6. The plug flow velocity distribution remains unchanged throughout the exchanger channels.

The above idealizations are familiar and need little discussion. The first four idealizations are reasonable in most heat exchanger applications. The fifth idealization has been shown to be valid for a variety of special cases when Peclet numbers are larger than 50 [10, 11], it seems reasonable to assume that this idealization is valid for the particular cases of interest here where the Peclet number exceeds 50. The sixth idealization is related to the plug flow assumption for the fluids. This is, however an accurate assumption when the Peclet number is less than 50 [10, 11]. We used this assumption for mathematical simplicity, but finally, in order to alleviate this difficulty, an approximation technique will be presented which increases the Peclet number range over which the use of a plug flow model can be expected to give fairly accurate results for turbulent flow.

1. PROBLEM FORMULATION [Q1]

The double-pipe heat exchanger consists of channels separated by a common wall with fluids flowing through the channels, as illustrated in Fig. 1.

Based on the previous simplifications, the energy conservation and the Fourier law of heat conduction, for the heat exchanger channels shown in Fig. 1, are as follows:

$$u_1 \frac{\partial T_1}{\partial z} = \alpha_1 \frac{\partial}{\partial r_1}\left(\frac{1}{r_1}\frac{\partial T_1}{\partial r_1}\right), \tag{4}$$

$$u_2 \frac{\partial T_2}{\partial z} = \alpha_2 \frac{\partial^2 T_2}{\partial {r_2}^2}, \tag{5}$$

where $\alpha \frac{k}{\rho c}$, u_1 and u_2 are the absolute values of velocity. The boundary conditions are

$$\mathrm{r_i} = 0: \qquad \frac{\partial T_i}{\partial r_i} = 0 \tag{6}$$

$\mathrm{r_i} = \mathrm{a_i}$:

$$q_1 + q_2 = 0 \quad \Rightarrow$$

$$2\pi k_1 L a_1 \frac{\partial T_1}{\partial r_1} + 2\pi k_2 L a_2 \frac{\partial T_2}{\partial r_2} = 0. \tag{7}$$

The heat balance equation at the interface of fluid 1 and the wall ($r_1 = a_1$) is

$$q_1 = q_w \quad \Rightarrow$$

$$2\pi k_1 a_1 \left.\frac{\partial T_1}{\partial r_1}\right|_{r_1=a_1} = 2\pi k_w \frac{T_2(a_2, z) - T_1(a_1, z)}{Ln(\frac{a_1+b}{a_1})}. \tag{8}$$

Equations (4) and (5) are special cases of the two-region Sturm–Liouville problem.

2. DIMENSIONLESS EQUATIONS

The dimensionless space variables are defined as follows:

For inner tube 1:

$$R_1 = \frac{r_1}{a_1}. \tag{9a}$$

For outer tube 2:

$$R_2 = \frac{r_2}{a_2}. \tag{9b}$$

The dimensionless length Z for tubes 1 and 2, referenced arbitrarily to the properties of tube 1, is defined as

$$Z = \frac{4}{Pe_1} \left(\frac{z}{2a_1}\right) , \tag{10}$$

where Pe_1 is the Peclet number for the inner tube defined as $\mathrm{Pe}_1 = \frac{2a_1u_1}{\alpha_1}$. The inverse of Z is proportional to the Graetz number. Other dimensionless parameters are

$$H = \frac{c_2 M_2}{c_1 M_1},\ K = \frac{k_1 a_2}{k_2 a_1}\left(1+\left(\frac{b}{a_1}\right)\right)^{-1},$$
$$K_W = \frac{k_1 b'}{k_w a_1}, b' = a_1 Ln\left(1+\frac{b}{a_1}\right) \tag{11}$$

and

$$\psi^2 = \frac{1}{2} KH .$$

The dimensionless temperature for the inner and outer tube sides is defined as

$$\theta_1(X_1, Z) = \frac{T_1 - T_{c(in)}}{T_{h(in)} - T_{c(in)}}, \tag{12}$$

$$\theta_2(X_2, Z) = \frac{T_2 - T_{c(in)}}{T_{h(out)} - T_{c(in)}}. \tag{13}$$

The governing equations in terms of the dimensionless variables θ_i, R_i, and Z are:

For the inner tube:

$$\frac{\partial \theta_1}{\partial Z} = \frac{1}{R_1}\frac{\partial}{\partial R_1}\left(R_1 \frac{\partial \theta_1}{\partial R_1}\right). \tag{14}$$

For the outer tube:

$$\frac{\partial \theta_2}{\partial Z} = \psi^2 \frac{\partial^2 \theta_2}{\partial {R_2}^2}. \tag{15}$$

Boundary conditions:

$$\theta_1(R_1, 0) = 0 \ , \tag{16}$$

$$\theta_2(R_2, 0) = 0 \ , \tag{17}$$

$$R_i = 0: \quad \frac{\partial \theta_i}{\partial R_i} = 0, \tag{18}$$

$$R_i = 1: \quad K\frac{\partial \theta_1}{\partial R_1} + \frac{\partial \theta_2}{\partial R_2} = 0, \tag{19}$$

$$R_i = 1: \quad K_W \frac{\partial \theta_1}{\partial R_1} + \theta_1(1,Z) - \theta_2(1,Z) = 0. \tag{20}$$

3. SOLUTION

To solve the problem, separation of variables is used; for channel 1 separation in the following form is assumed:

$$\theta_I(R_1, Z) = N(Z)M_1(R_1) \; . \tag{21}$$

Applying Eq. (21) to Eq. (14) yields

$$\frac{M_1^{''}(R_1)}{M(R_1)} = \frac{N^{'}(Z)}{N(Z)} = -\lambda_n^2, \tag{22}$$

where λ_n is the eigenvalue, and

$$\frac{N^{'}(Z)}{N(Z)} = -\lambda_n^2 \quad \Rightarrow \quad N(Z) = e^{-\lambda_n^2 Z}. \tag{23}$$

Thus

$$\theta_1(R_1, Z) = \sum_{n=0}^{\infty} C_n M_{1n}(R_1) e^{-\lambda_n{}^2.Z}. \tag{24}$$

A similar method applied to Eq. (5) gives

$$\theta_2(R_2, Z) = \sum_{n=0}^{\infty} C_n M_{2n}(R_2) e^{-\lambda_n{}^2.Z}. \tag{25}$$

Applying the new variables θ_1 and θ_2 into Eq. (14) and Eq. (15) yields

$$\frac{1}{R_1}\frac{\partial}{\partial R_1}\left(R_1 M_{1n}^{'}\left(R_1\right)\right) + \lambda_n^2 M_{1n}(R_1) = 0, \tag{26}$$

$$M_{2n}^{''}(R_2) + \psi^2 \lambda^2 M_{2n}(R_2) = 0. \tag{27}$$

Applying the new variables θ_1 and θ_2 into Eqs. (18) to (20) gives

$$M_{1n}^{'}(0) = 0, \tag{28}$$

$$M'_{2n}(0) = 0, \tag{29}$$

$$K.M'_{1n}(1) + M'_{2n}(1) = 0, \tag{30}$$

$$K_W.M'_{1n}(1) + M_{1n}(1) - M_{2n}(1) = 0. \tag{31}$$

3.1. Eigenvalue Equation

Assuming M_{1n} (R_1) =A.F (λ_n, R_1) and M_{2n} (R_2) = B.G (λ_n, R_2), where A and B are arbitrary constants, Eq. (30) and Eq. (31) become

$$KAF_{R_1}(\lambda_n,1) + BG_{R_2}(\lambda_n,1) = 0. \tag{32}$$

$$A[K_W F_{R_1}(\lambda_n,1) + F(\lambda_n,1)] - BG(\lambda_n,1) = 0. \tag{33}$$

In order for this system of simultaneous homogeneous linear algebraic equations to have nonzero solutions for A and B, the coefficient determinant must be made equal to zero by a proper choice of λ. This gives the eigenvalue equation

$$\begin{aligned} &F(\lambda_n,1)G_{R_2}(\lambda_n,1) + KF_{R_1}(\lambda_n,1)G(\lambda_n,1) \\ &+K_W F_{R_1}(\lambda_n,1)G_{R_2}(\lambda_n,1) = 0. \end{aligned} \tag{34}$$

Equation (32) gives

$$B = -KA\frac{F_{X_1}(\lambda,1)}{G_{X_2}(\lambda,1)}. \tag{35}$$

Since the system is homogeneous, either A or B can be chosen arbitrarily. Hence

$$A = G_{X_2}(\lambda, 1) \tag{36}$$

The eigenfunctions M_{1n} and M_{2n} can be represented by

$$\begin{aligned} &M_{1n}(R_1) = AF(\lambda_n, R_1) = \\ &G_{R_2}(\lambda_n,1)F(\lambda_n, R_1), \end{aligned} \tag{37}$$

$$\begin{aligned} &M_{2n}(R_2) = BG(\lambda_n, R_2) = \\ &-KF_{R_1}(\lambda_n,1)G(\lambda_n, R_2). \end{aligned} \tag{38}$$

3.2. Finding $F(\lambda_n, X_1)$ and $G(\lambda_n, X_2)$

The solution for Eq. (26) along with the boundary condition, Eq. (28), is

$$M_{1n}(R_1) = AF(\lambda_n, R_1) = AJ_0(\lambda_n R_1). \tag{39}$$

Thus **[Q12]**

$$M_{1n}(R_1) = -\psi\lambda_n \sin(\psi\lambda_n) J_0(\lambda_n R_1), \tag{41}$$

$$M_{2n}(R_2) = K\lambda_n J_1(\lambda_n)\cos(\psi\lambda_n R_2). \tag{42}$$

3.3. Orthogonality of the Eigenfunctions

The equivalent of an orthogonality condition for M_{1n} and M_{2n} will now be established. Equation (26) is first manipulated for $n = i$ and j in the same manner used to derive the properties of the familiar Sturm–Liouville system. For example, Eq. (26) is written for $n = i$ and then for $n = j$ with $i \neq j$. The equation for $n = i$ is multiplied by M_{1j} and the equation for $n = j$ is multiplied by M_{1i}. The resulting equations are subtracted, simplified, and then integrated between $R_1 = 0$ and $R_1 = 1$. The following equation results:

$$\left(\lambda_j^2 - \lambda_i^2\right)\int_0^1 R_1 M_{1j}(R_1) M_{1i}(R_1)\,dR_1 = M_{1j}(1)M_{1i}'(1) - M_{1i}(1)M_{1j}'(1). \tag{43}$$

In a similar manner Eq. (27) gives

$$\psi^2\left(\lambda_j^2 - \lambda_i^2\right)\int_0^1 M_{2j}(R_2) M_{2i}(R_2)\,dR_2 = M_{2j}(1)M_{2i}'(1) - M_{2i}(1)M_{2j}'(1). \tag{44}$$

The integrals of Eq. (44) can be related to each other using the coupling boundary conditions at $R = 1$. Thus, Eq. (30) gives

$$M_{2n}'(1) = -KM_{1n}'(1), \tag{45}$$

and Eq. (31) gives

$$M_{2n}(1) = M_{1n}(1) + K_W M_{1n}'(1). \tag{46}$$

Using these conditions in Eqs. (43) and (44) gives

$$\int_0^1 \begin{matrix} 2R_1 M_{1i}(R_1) M_{1j}(R_1) dR_1 \\ + \int_0^1 HM_{2j}(R_2) M_{2i}(R_2) dR_2 = 0. \end{matrix} \tag{47}$$

Equation (47) is the equivalent of an orthogonality for the eigenfunctions M_{1n} and M_{2n} for the case of $i = j = n$ and leads to a normalizing factor defined by

$$N_n = \int_0^1 2R_1 M_{1n}^2(R_1) dR_1 + \int_0^1 HM_{2n}^2(R_2) dR_2 = 0. \tag{48}$$

For the case of $n = 0$ with $\lambda_0 = 0$, $M_{10} = M_{20} = 1$ must be included. Also, application of Eq. (48) gives

$$N_0 = 1 + H\ . \tag{49}$$

3.4. Finding C_n

Consider the following expansions regarding Eqs. (24) and (25) at $Z = 0$

$$0 = \sum_{n=0}^{\infty} C_n M_{1n}(R_1), \tag{50}$$

$$1 = \sum_{n=0}^{\infty} C_n M_{2n}(R_2). \tag{51}$$

Multiplying Eq. (50) by $2R_1M_{1n}(R_1)dR_1$ and Eq. (51) by $HM_{2n}(X_2)dX_2$, adding the resulting expressions and integrating between $R_i = 0$ and $R_i = 1$ using Eq. (48), the following equation for C_n results:

$$C_n = \frac{1}{N_n} \int_0^1 HM_{2n}(R_2) dR_2. \tag{52}$$

Equations (49) and (52) give

$$C_0 = \frac{H}{N_0} = \frac{H}{1+H}. \tag{53}$$

3.5. Plug Flow Solutions

Analytical solutions for the mathematical problem specified by Eqs. (14) to (20) will now be discussed briefly. Solution for the dimensionless temperature distribution can be written as

$$\theta_i(R_i, Z) = \frac{H}{1+H} + \sum_{n=0}^{\infty} Q_{in}(R_i) e^{-\lambda_n{}^2 . Z} \qquad i = 1,2 . \tag{54}$$

In this equation, $Q_{in}(R_i)$ are the functions of an eigenvalue λ_n and the dimensionless distance variable R_i. The eigenvalues are the positive nonzero roots of an eigenvalue equation from Eq. (34):

$$F(\lambda) = \sqrt{\frac{2K}{H}} J_1(\lambda) \cos(\psi\lambda) + J_0(\lambda) \sin(\psi\lambda) - K_W \lambda J_1(\lambda) \sin(\psi\lambda) = 0. \tag{55}$$

The functions $Q_{in}(R_i)$ for the concentric tube heat exchangers when one recalls from Fig. 1 that channel 1 identifies the circular tube and that channel 2 refers to the narrow annular space are

$$Q_{1n} = \frac{2 \sin(\psi\lambda_n) J_0(\lambda_n R_1)}{\lambda F'(\lambda_n)} \tag{56}$$

and

$$Q_{2n} = -\frac{2KJ_1(\lambda_n) \cos(\psi\lambda_n R_2)}{\psi\lambda_n F'(\lambda_n)}, \tag{57}$$

where $F'(\lambda_n)$ represents the derivative of $F(\lambda_n)$ with respect to λ.

3.6. Heat-Transfer Coefficient

The local tube side heat-transfer coefficient is defined in the usual manner, which in dimensionless form, becomes

$$Nu_i(Z) = \frac{2 \left.\frac{\partial \theta_i}{\partial R_i}\right|_{R_i=1}}{\theta_i(1, Z) - \theta_{AVi}(Z)}, \tag{58}$$

where

$$\theta_{AV1}(Z) = 2\int_0^1 R_1 \theta_1(R_1, Z) dR_1, \tag{59}$$

and

$$\theta_{AV2}(Z) = \int_0^1 \theta_2(R_2, Z) dR_2. \tag{60}$$

3.7. An Approximation for Turbulent Flow

The basis for the approximation is described for the case of turbulent convection heat transfer for flow through a concentric tube. The appropriately simplified convection heat transfer equation for turbulent flow is

$$\frac{\partial}{\partial R}\left[\left(k + c\rho\varepsilon\right)\frac{\partial T}{\partial R}\right] = c\rho u \frac{\partial T}{\partial Z}, \tag{61}$$

where the dimensionless distance variable R ($0 \le X_R \le 1$) has been used, and subscripts have been dropped for convenience. In this equation, ε represents a turbulent diffusivity for heat transfer. The term $k + c\rho\varepsilon$ can be interpreted as an effective total conductivity k_t, and is written as

$$k_t = k\left(1 + \frac{\varepsilon}{v}\mathrm{Pr}\right), \tag{62}$$

where v is the kinematics viscosity and Pr is the Prandtl number. Now an average effective conductivity k_m is defined by

$$k_m = \int_0^1 k_t dR. \tag{63}$$

The k_m approximation for a double pipe heat exchanger was tested by comparing k_m values computed from Eq. (63) with the fully developed turbulent flow by Lyon [12] and Shimazaki [13] as

$$k_m = \frac{k}{5.8}\left(0.02 + \mathrm{Re}^{0.8}\,\mathrm{Pr}^{0.75}\right). \tag{64}$$

The average effective conductivity, k_m, must be applied to the double-pipe heat exchanger problem of this paper; plug flow results as obtained from solutions to the mathematical problem described by Eq. (11) can be converted to the turbulent flow results using Eq. (63) with K and K_W now being defined as follows:

$$K_t = \frac{k_{m1}a_2}{k_{m2}a_1}\left(1 + \left(\frac{b}{a_1}\right)\right)^{-1}, \quad K_W = \frac{k_{m1}b'}{k_w a_1}. \tag{65}$$

4. RESULTS

The results are compared with the established experimental data available in the literature using similar pipe dimensions and flow details [9]. The exchanger geometrical data are shown in Table 1. The working fluid is water at atmospheric pressure. Temperature was measured at the inlet and outlet of the two streams and also at an

Table 1
The exchanger geometrical data

The inner tube inner diameter	16.5 mm
The inner tube outer diameter	21.5 mm
The outer tube inner diameter	27.5 mm
The inner tube height	650 mm
The outer tube height	600 mm
Total exchanger length	1500 mm
External tube area	0.10 mm
The tube material	Steel

Table 2
Inner and outer tube heat transfer properties

		μ (kg/m·sec) $\times 10^6$	Re	Pr	k (Wm^{o}C)
1	Outer tube	863	1265	5.93	0.6107
	Inner tube	480	11,510	3.08	0.6530
2	Outer tube	850	1131	5.82	0.6116
	Inner tube	480	11,510	3.08	0.6530
3	Outer tube	822	1326	5.62	0.6145
	Inner tube	439	12,585	2.80	0.6580
4	Outer tube	863	1475	5.93	0.6107
	Inner tube	466	11,856	2.99	0.6550

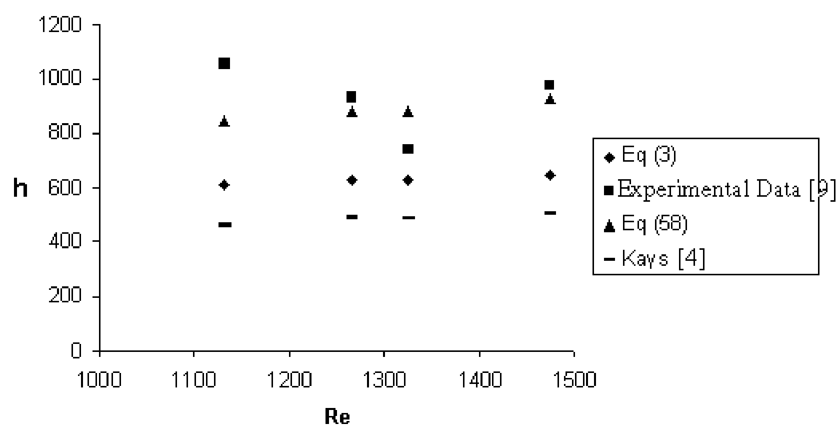

Fig. 2. The outer tube side heat-transfer coefficient.

Table 3
Temperature distribution, T_E: Experimental data [9], T: Local temperature of the double-pipe heat exchanger from Eqs. (59) and (60) with turbulent approximation

	T_{Eh1} (°C)	T_{Eh2} (°C)	T_{h2} (°C)	T_{Ehm} (°C)	T_{hm} (°C)	W_h (kg/sec)
1	63.7	57.3	59.2	60.1	61.7	0.72
2	64.4	57.5	59.9	60.4	62.4	0.72
3	68.4	62.6	63.3	66.3	66.4	0.72
4	66.1	58.9	61.0	62.2	63.9	0.72
	T_{Ec1} (°C)	T_{Ec2} (°C)	T_{c2} (°C)	T_{Ecm} (°C)	T_{cm} (°C)	W_c (kg/sec)
1	22.3	32.3	30.1	27.2	27.8	0.042
2	21.7	33.6	30.5	27.8	27.9	0.037
3	26.9	35.7	34.7	30.1	32.4	0.042
4	21.5	31.6	29.0	26.9	26.8	0.049

intermediate point half way between the inlet and outlet by Mehrabian and Mansouri [9]. **[Q2]** The heat-transfer coefficients are interfered from the measured data.

Calculating the temperature distribution and film heat-transfer coefficient for the tube side flows requires one to know viscosity, Reynolds number, Prandtl number, and conductivity of water. These data for the inner and outer tubes are listed in Table 2. The results are listed in Table 3 for comparison with the experimental data of Mehrabian and Mansouri [9].

The outer tube side heat-transfer coefficient based on the analytical solution of Eq. (58), experimental data, and standard correlation are listed in Table 4. Also, the comparison is illustrated in Fig. 2.

Table 4
Comparsation between the analytical solution based on Eq. (58), experimental data, and standard correlation

	h_0 [W/m^2, °C] Eq. (58)	h_0 [W/m^2, °C] Experimental data [9]	h_0 [W/m^2, °C] Eq. (3)	h_0 [W/m^2, °C] Kays [4]
1	881.5	933	624	489
2	846	1054	607.2	459
3	881	741	626.4	481
4	927.5	974	646.8	499

CONCLUSIONS

The outer tube side heat-transfer coefficients deduced from Eq. (58) are compared with experimental data and those are evaluated based on standard correlations. All standard correlations predict lower heat-transfer coefficients compared with the experimental data and the analytical solution. The Sider–Tate [7] correlation predicts the highest values among other standard correlations. The discrepancy may be because of the standard correlations which are, generally, presented for the smooth heat transfer surface, while in a real exchanger the heat transfer surfaces are not smooth and this results in higher heat transfer; where Eq. (64) interferes this effect to our solution. The mathematical model of the heat transfer phenomenon in a double-pipe heat exchanger with parallel flow has been developed and investigated theoretically in this study. The analytical solution is obtained based on a two region Sturm–Liouville system consisting of two equations coupled at a common boundary. In order to provide mathematical simplicity, plug flow models of the heat exchanging fluids were utilized for analysis and an approximation method was developed for application of plug flow resulting in general to the turbulent flow conditions. The mathematical method performed in this study can be applied to prediction of the temperature distribution in one or two-dimensional form.

NOMENCLATURE

a_1	radius of inner pipe 1, m
$a_2/2$	radius of outer pipe 2, m
b	wall thickness, m
c_i	heat capacity of fluid i, J/kg·K
k_i	thermal conductivity of fluid i, W/m·K
k_w	thermal conductivity of wall, W/m·K
k_t	thermal conductivity for turbulent flow, W/m·K
k_m	average effective conductivity, W/m·K
q_i	heat-flux density at the wall in channel i, W/m^2
r	coordinate normal to the heat transfer surface, m
T_i	local temperature of fluid i, $^\mathrm{o}$C
T_c(in)	inlet temperature for channel 1, $^\mathrm{o}$C
T_h(in)	inlet temperature for channel 2, $^\mathrm{o}$C
T_h(out)	outlet temperature for channel 2, $^\mathrm{o}$C
u_i	velocity of fluid i
z	axial coordinate or heat exchanger length, m

Greek symbols

α_i	thermal diffusivity of fluid i, m^2/sec
ε	turbulent diffusivity for heat transfer, m^2/sec
λ	eigenvalue
ν	kinematic viscosity, m^2/sec

Dimensionless quantities

H	heat capacity flow rate ratio
K	relative thermal resistance of fluid
K_W	relative thermal resistance of wall
Pe	Peclet number
Pr	Prandtl number
Re	Reynolds number
θ_i	local temperature of fluid *i*
R	dimensionless radius
Z	dimensionless length
$\dot{M}$	mass flow rate of fluid, kg/sec

Subscripts

B	bulk temperature
c	cold
h	hot
i	channel, $i = 1$ or 2
m	0 for parallel flow, 1 for counter flow
n	0, 1, 2, 3, ...
t	turbulent.

REFERENCES

1. Shah, R. K. and London, A. L. Laminar Flow Forced Convection in Ducts. A Source Book for Compact Heat Exchanger Analytical Data, *Advances in Heat Transfer*, Academic Press, New York, 1978.
2. Short, B. E. *Heat Transfer and Pressure Drop in Heat Exchangers*, Univ. Texas Publ., 1943, No. 4324, pp. 1–5.
3. Abdelmessih, A. N. and Bell, K. J. Effect of Mixed Convection and U-Bend on the Design of Double Pipe Heat Exchangers, *Heat Transfer Eng.*, 1999, Vol. 20, No. 3, **[Q3]**.
4. Kays, W. M. *Convective Heat and Mass Transfer*, McGraw-Hill, New York, 1966, pp. 187–190.
5. Sellars, J. R., Tribus, M., and Klein, G. S. Heat Transfer to Laminar Flows in a Round Tube or Flat Conduit: The Graetz Problem Extended, *Trans. ASME*, 1956, Vol. 78, pp. 441-**[Q4]**.
6. Holman, J. P. *Heat Transfer*, 8th ed., McGraw-Hill, New York, **[Q5]**.
7. Sieder, E. N. and Tate, F. E. Heat Transfer and Pressure Drop in Tube, *Ind. Eng. Chem.*, 1936, Vol. 28, pp. 1429–1436.
8. Kern, D. Q. *Process Heat Transfer*, McGraw-Hill, New York, 1950.
9. Mehrabian, M. A. and Mansouri, S. H. The Overall Heat Transfer Characteristics of Double Pipe Heat Exchanger: Comparison of Experimental Data with Predictions of Standard Correlation, *IJE Trans.*, 2002, Vol. 15, pp. 395–405.

10. Eckert, E. R. *Heat and Mass Transfer*, McGraw-Hill, New York, 1959, pp. 298–301.
11. Poppendiek, H. F. **[Q6]**, *Nucl. Sci. Eng.*, 1959, Vol. 5, pp. 390-**[Q7]**.
12. Lyon, R. **[Q8]**, *Chem. Eng. Progr.*, 1951, Vol. **[Q9]**, pp. 47–75.
13. Shimazaki, T. **[Q10]**, *Chem. Eng. Progr.*, 1951, Vol. 73, pp. 803-**[Q1]**.

□◆◆◆□

[Q1] AU: Is numbering of sections OK ? Please check

[Q2] AU: Do you mean this reference ?

[Q3] AU: Please indicate the page range.

[Q4] AU: Please indicate the final page.

[Q5] AU: Please indicate the year.

[Q6] AU: Please give the article title.

[Q7] AU: Please indicate the final page.

[Q8] AU: Please give the article title.

[Q9] AU: Please indicate the volume.

[Q10] AU: Please give the article title.

[Q11] AU: Please indicate the final page.

[Q12] AU: Please check numbering of Equations. Eq. (40) is missing.